Injection-induced, tunable all-optical gating in a two-state quantum dot laser

Article *in* Optics Letters · August 2016

DOI: 10.1364/OL.41.003555

9 authors, including:

Stephen P. Hegarty

Cork Institute of Technology

129 PUBLICATIONS **1,021** CITATIONS

SEE PROFILE

Guillaume Huyet

Cork Institute of Technology

265 PUBLICATIONS **2,615** CITATIONS

SEE PROFILE

David Goulding

Cork Institute of Technology

54 PUBLICATIONS **352** CITATIONS

SEE PROFILE

Injection-induced, tunable, all-optical gating in a two-state quantum dot laser

E.A. Viktorov[1,2], I. Dubinkin[1], N. Fedorov[1], T. Erneux[2], B. Tykalewicz[3,4], S.P. Hegarty[3,4], G. Huyet[1,3,4], D. Goulding[3,4], and B. Kelleher[4,5,*]

[1]National Research University of Information Technologies, Mechanics and Optics, Saint Petersburg, Russia
[2]Optique Nonlinéaire Théorique, Université Libre de Bruxelles, Bruxelles, Belgium
[3]Centre for Advanced Photonics and Process Analysis (CAPPA), Cork Institute of Technology, Cork, Ireland
[4]Tyndall National Institute, National University of Ireland, University College, Cork, Ireland
[5]Department of Physics, University College Cork, Cork, Ireland
[*]Corresponding author: bryan.kelleher@ucc.ie

Compiled July 2, 2016

We demonstrate a tunable all-optical gating phenomenon in a single section quantum dot laser. The free-running operation of the device is emission from the excited state. Optical injection into the ground state of the material can induce a switch to emission from the ground state with complete suppression of the excited state. If the master laser is detuned from the ground state emitting frequency, a periodic train of ground state dropouts can be obtained. These dropouts act as gates for excited state pulsations: during the dropout the gate is opened and gain is made available for the excited state and the gate is closed again when the dropout ends. Numerical simulations using a rate equation model are in excellent agreement with experimental results.

OCIS codes: *(140.3540) Lasers, Q-switched; (140.3520) Lasers, injection-locked; (190.1450) Bistability; (250.5590) Quantum-well, -wire and -dot devices*

http://dx.doi.org/10.1364/ao.XX.XXXXXX

The most common techniques to produce pulse trains from lasers are mode-locking, used to obtain ultrafast pulses, and Q-switching, used to deliver high energy pulses. Conventional Q-switched operations rely on either active or passive modulation of losses. In a passive configuration the gating process is typically provided by an intracavity absorber. In order to obtain the desired pulsating outputs, the absorber must be saturable so that the losses are reduced at high optical intensities. Moreover, the losses need to recover quickly to maintain pulsed operation and avoid a continuous output [1]. In the passive configuration the repetition rate is controlled by the pumping of the device. With a view to all-optical functionality and signal processing [2–4], a tunable all-optical gating technique is desirable.

Unlike most conventional semiconductor lasers, quantum dot (QD) lasers may operate at distinct energy states. Depending on the temperature and pumping, single state emission from either the ground state (GS) or the first excited state (ES) is possible as well as simultaneous two-state lasing from both the GS and first ES [5, 6]. Traditionally, studies have focussed on the GS properties of QD lasers. However, recently interest has grown in analysing the ES properties particularly with a view to applications [7–9]. In [9] we reported on all-optical switching between the two states via optical injection. All-optical switching can be obtained in several other laser systems such as VCSELs [10, 11], two-mode edge emitting lasers [12], semiconductor ring lasers [13] and DFB QD lasers [14]. In this letter, we report on a gating effect provided by optical injection into a QD laser strongly pumped so that it is emitting from the ES only. We have recently found bistable transitions between GS and ES emissions in the same experimental setup [7]. The bistability phenomenon leads to a hysteresis loop for the lasing output when the injected light power is swept up and down close to the wavelength of the GS. Here we find that a Q-switched pulse train emerges from a homoclinic bifurcation at the edge of the hysteresis loop where GS phase locking breaks down. Beyond this bifurcation the GS still emits light but is now unlocked from the master laser (ML). The unlocked GS saturates fast which allows it to act as an effective gate in the system. Unlike the conventional Q-switching scenario, modulation of losses is not required. Here, the physical mechanism leading to pulsating intensities is different because a single section acts as both an amplifier and a gate due to distinct energy states.

The slave laser (SL) was a 0.6 mm long InAs based QD laser similar to that used in [9]. The emission from the GS was on a single longitudinal mode at approximately 1300 nm and the ES emission was multimode with a spectral width of approximately 10 nm centred close to 1220 nm [15]. At a temperature of 20° C there were three distinct regimes: the threshold to GS only lasing was at 34 mA, at 60 mA lasing occurred from both the GS and the ES simultaneously and above 80 mA emission was from the ES only. Such an evolution has been previously reported both experimentally and theoretically [5, 6, 9, 16, 17].

The experimental arrangement is identical to that presented in [7]. The ML was a commercially available tunable laser, tunable in steps of 0.1 pm and with a linewidth less than 100 kHz.

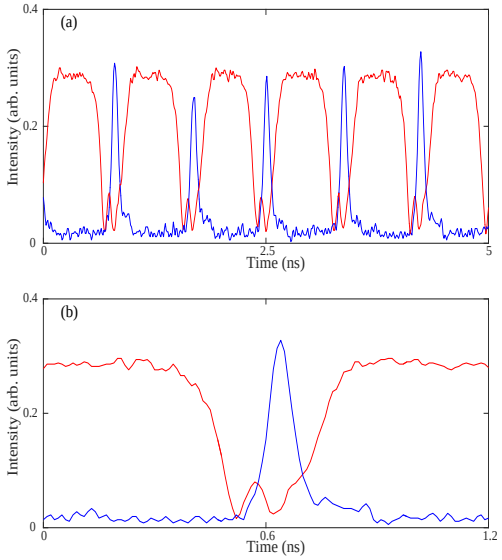

Fig. 1. (Color online) (a) Experimental time trace showing time-periodic large-amplitude ES pulses (blue) together with periodic GS dropouts (red). (b) shows a zoom of one of the dropouts / pulsations.

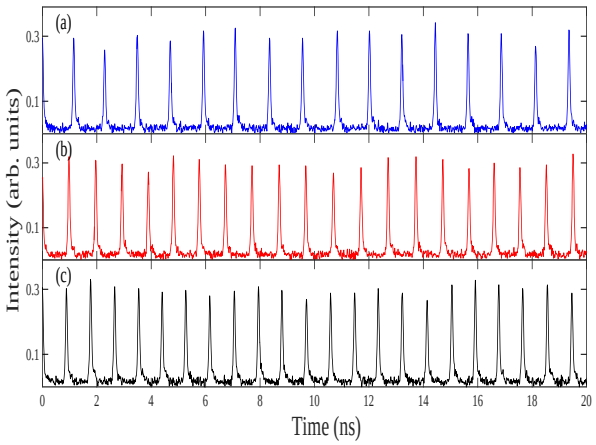

Fig. 2. (Color online) Evolution of the pulse trains as the frequency of the master laser is varied. For (a) the detuning is -890 MHz. The master frequency is decreased by approximately 270 MHz from (a) to (b) and again from (b) to (c). The repetition rate increases by approximately 110 MHz from (a) to (b) and by approximately 150 MHz from (b) to (c).

The ML was coupled to the SL via an optical circulator and lensed fibre. A polarization controller was used to ensure maximal coupling of the light from the ML to the SL. Tunable filters allowed both independent and simultaneous analysis of the GS and ES signals. The outputs were finally analyzed on a high speed, real-time oscilloscope. The SL was electrically pumped at 84 mA at which point it emitted from the ES with a suppression ratio of greater than 30 dB over the GS output. The wavelength separation between the two states at this operating point was $\sim$ 85 nm which corresponds to $\sim$ 16 THz. By injecting from the ML into the GS with sufficient strength and appropriate detuning, the GS could be made to lase with the ES suppressed by approximately 40 dB over its free-running value.

In our previous work [7], we fixed the wavelength of the ML to give the maximum CW phase-locked intensity of the GS and swept the injection power of the ML up and down. As a result, we obtained a bifurcation diagram exhibiting injection induced hysteresis but no pulsating regimes. Here, we fix the injection power and vary the detuning and find dynamical instabilities as the detuning is changed towards higher ML frequencies. The nature of these instabilities depends on the strength of the ML. In this work, we consider moderately high levels of injection with approximately 250 μW of ML power reaching the facet of the SL. Unlike the single mode injection system, identifying the detuning is difficult here since the GS does not lase in the absence of injection. Thus, we express our experimental detuning relative to the frequency at which the GS intensity is maximised as previously used in [7]. Figure 1 shows an example of the GS and ES intensities at a detuning of approximately -1.51 GHz. A periodic train of ES pulses appears together with periodic GS dropouts. The ES pulses are quite short with widths of approximately 80 ps. The dropouts in the GS are significantly longer. Small amplitude oscillations in the GS intensity are observed during the low intensity part of the dropouts. In the case shown this is manifest as one clear oscillation before the return to the high intensity GS output. As the frequency of the ML was progressively decreased, the period of the pulse train increases suggesting that we approach a homoclinic bifurcation as in the case of the single mode laser with a saturable absorber [1]. We note that in [18] picosecond ES pulses were obtained theoretically in a similar scheme. There are several important differences with this work. Most importantly, the behavior of the GS was significantly different with very slow evolution of the GS intensity in [18] rather than the very fast intensity dropouts we obtain. The intensities of the two states were also very different in [18].

Figure 2 shows frequency tuning of the repetition rate via master laser tuning.In principle, as the detuning approaches the homoclinic bifurcation, the period tends to infinity and thus the frequency tends to zero. However, in reality noise plays a major role and in particular, the very low frequency trains are subject to significant jitter. Thus, while very low repetition rates can be obtained in the experiment but they are significantly aperiodic. If we focus only on low jitter trains then we find a tuning range of approximately 1 GHz (from approximately 0.3 GHz to approximately 1.3 GHz) . To put this into perspective, we can compare it with the tuning ranges of passively mode locked QD lasers when subject to dual mode injection [19], hybrid mode locked QD lasers subject to single mode optical injection [19] and mode locked QD lasers subject to dual feedback [20]. In each of these cases, tuning ranges on the order of two or three hundred MHz were obtained. Our straightforward control of a such a wide range of repetition rates could be valuable for all-optical processing and is in direct contrast to the typical passive Q-switching configuration where only extremely limited tuning is possible since the rate is primarily set by the pump and the absorber time scales.

To identify the underlying mechanism, we investigate the bifurcation diagram for the GS and ES intensities using appropriate rate equations. We consider the dimensionless rate equation model for QD lasers introduced in [7]. It consists of five equations for the complex electric field of the GS (E_g), the intensity of the ES (I_E), the occupation probabilities of the GS (n^g) and ES (n^e) and the carrier density in the wetting layer (n^w). The

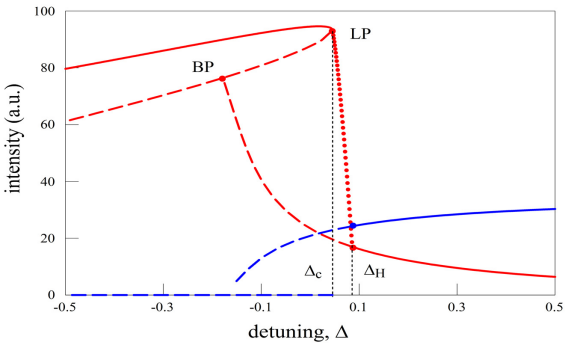

Fig. 3. (Color online) Numerical bifurcation diagram. GS (red) and ES (blue) intensities vs detuning Δ. Continuous (dashed) lines correspond to stable (unstable) branches. Δ_c and Δ_H denote a homoclinic bifurcation point and a Hopf bifurcation point, respectively. The dotted red line shows the time average of the periodic GS pulse intensities. From left to right the single mode GS steady state is followed by a branch of time-periodic intensities starting at the limit point LP and terminating at the Hopf bifurcation point Δ_H. BP denotes an unstable bifurcation point. If $\Delta > \Delta_H$, the GS-ES steady state is the only attractor. The fixed parameters are: $\eta = 0.01$, $\varepsilon = 3$, $\alpha = 3$, $\beta = 2.4$, $g_0^g = g_0^e = 0.55$, $J = 40$, $B_{e,h} = B_{e,h}^w = 100$, $C_e^w = 10$, $C_h^w = 10^2$, $C_e = B_e \exp(-2)$, $C_h = B_h$ [7].

equations are

$$\dot{E}_g = \frac{1}{2}[(1+i\alpha)(2g_0^g(n_e^g + n_h^g - 1) - 1) + i4\beta g_0^e(n_e^e + n_h^e - 1)]E_g + i\Delta E_g + \epsilon, \quad (1)$$

$$\dot{I}_e = [4g_0^e(n_e^e + n_h^e - 1) - 1]I_e, \quad (2)$$

$$\dot{n}_{e,h}^g = \eta[2B_{e,h}n_{e,h}^e(1 - n_{e,h}^g) - 2C_{e,h}n_{e,h}^g(1 - n_{e,h}^e) - n_e^g n_h^g - g_0^g(n_e^g + n_h^g - 1)I_g], \quad (3)$$

$$\dot{n}_{e,h}^e = \eta[-B_{e,h}n_{e,h}^e(1 - n_{e,h}^g) + C_{e,h}n_{e,h}^g(1 - n_{e,h}^e) + B_{e,h}^w n_{e,h}^w(1 - n_{e,h}^e) - C_{e,h}^w n_{e,h}^e - n_e^e n_h^e - g_0^e(n_e^e + n_h^e - 1)I_e], \quad (4)$$

$$\dot{n}_{e,h}^w = \eta[J - n_e^w n_h^w - 4B_{e,h}^w n_{e,h}^w(1 - n_{e,h}^e) + 4C_{e,h}^w n_{e,h}^e]. \quad (5)$$

α is the usual phase-amplitude coupling/linewidth enhancement factor. g^g and g^e are gain coefficients for the ground and excited states respectively. The empirical term β is used to qualitatively introduce some of the effects of inhomogeneous broadening and enters the equations as a phase-amplitude coupling between the GS and the ES [7, 8]. ε is the injection strength and $\Delta = \omega_i - \omega_g$ is the detuning between the frequency of the injected light and that of the GS. J is the pump current and the terms $B_{e,h}$ and $B_{e,h}^w$ determine the capture rates to the GS and ES respectively. The C terms are escape rates linked to the capture rates B via a Kramers relation as described in [7] and with the same parameter values as in [7]. The model takes into account the differing spin degeneracies in the QD energy levels, Pauli blocking, and interstate captures and escapes. Our two primary control parameters are the injection strength ε and the detuning Δ defined as the difference between the frequency of the injected signal and that of the GS.

The pump current is adjusted so that the free-running emission ($\varepsilon = 0$) is from the ES only. The injection of light at a wavelength close to that of the GS leads to a hysteresis phenomenon for the lasing output when sweeping the ML power up and down. In order to describe our new experiments, we fix the injection strength and vary the detuning Δ. Figure 3 shows a typical bifurcation diagram for the GS and ES intensities. By progressively increasing Δ, we note a gradual increase of the GS intensity while the ES remains off. As Δ is further increased beyond a critical point Δ_c, the system exhibits a cycle that emerges from a homoclinic loop at the limit point of the GS branches (LP). The ES output is no longer zero but exhibits sustained periodic pulses as shown in Fig. 4 (a). The GS output, however, is very different and consists of nearly flat plateaux interrupted by large amplitude dropouts (see Fig. 4 (b)). As we further increase Δ the amplitude of the oscillations decreases and disappears at the Hopf bifurcation point $\Delta = \Delta_H$. This Hopf bifurcation point could be anticipated because the branch of stable ES states terminates at the unstable bifurcation point BP. Since the locations of all steady-state bifurcations and limit points are known, the change of stability of the ES branch is necessarily through a Hopf bifurcation point.

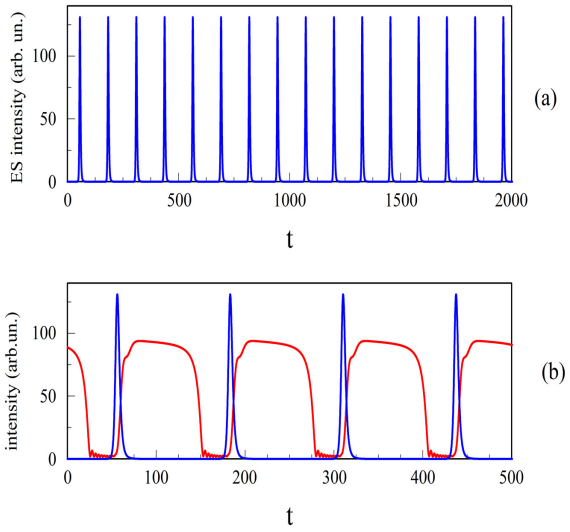

Fig. 4. (Color online) (a) Numerical time trace of large-amplitude Q-switched ES pulsations; (b) zoom of the pulses in (a) (blue) and the accompanying periodic GS dropouts (red). $\Delta = 0.06$. The other parameters are the same as in Fig. 3.

The physical mechanism leading to the strong ES pulses is reminiscent of the one responsible for the conventional Q-switching scenario in lasers with a saturable absorber. Figure 5 details the onset of one ES pulse. After the pulse, the GS recovers very fast and its gain saturates due to Pauli blocking (upper plateau). This saturation of the GS allows carriers to slowly build up in the ES. It acts as a gate allowing the ES carrier population to increase until it eventually overcomes the device losses. A short and intense ES pulse can then be emitted. The zoom allows us to observe the details and in particular the oscillations in the low intensity part of the GS output. These oscillations correspond physically to a beating between the GS and the injected light and indicate the proximity to a Hopf bifurcation similarly to the oscillation in the low intensity part of the GS dropout in the experiment.

This completes the Q-switched cycle. Note the small amplitude damped oscillations around the lower plateau of the GS before the ES pulse. Such oscillations are also observed in the

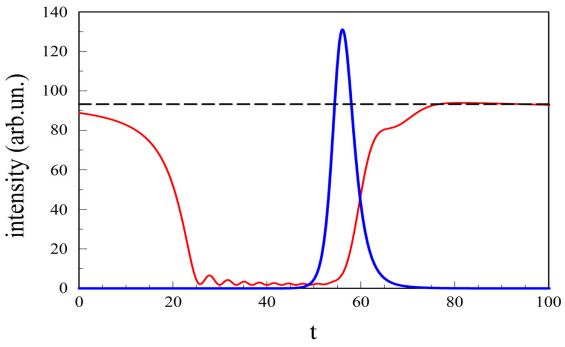

Fig. 5. (Color online) Numerical time trace showing a single large-amplitude Q-switched ES intensity pulse (blue) and the corresponding GS intensity dropout (red). The dashed line indicates the phase-locked GS intensity limit point. The fixed parameters are the same as in Fig. 3.

experiments (bottom time trace in Fig. 1). Physically they correspond to beating between the now unlocked GS output and the injected signal.

In conclusion, we have shown both experimentally and numerically how a Q-switched like operation is possible for an optically injected QD laser. It results from the two-state lasing capability of the laser. The injected and saturable GS operates as a gate for the ES output similar to how modulated losses open a gate in conventional Q-switching. Among the possible advantages of injection-induced gating is the simple control of the repetition rate by changing the injected frequency.

FUNDING INFORMATION

The authors acknowledge the INSPIRE programme funded by the Irish Government's Programme for Research in Third Level Institutions Cycle 5. The authors gratefully acknowledge the support of Science Foundation Ireland under Contract No. 12/RC/2276. The authors in Brussels acknowledge support of the Fonds National de la Recherche Scientifique (Belgium).

REFERENCES

1. T. Erneux and P. Glorieux, "Laser Dynamics", Cambridge University Press, Cambridge, UK, 2010.
2. H. Kawaguchi, *"Bistabilities and Nonlinearities in Laser Diodes,"* Artech House, Norwood, MA (1994)
3. M. J. Adams, A. Hurtado, D. Labukhin, and I. D. Henning, Chaos **20**, 037102 (2010).
4. I. White, R. Penty, M. Webster, Y. J. Chai, A. Wonfor, and S. Shahkooh, IEEE Commun. Mag., **40**, 74 (2002).
5. A. Markus, J. X. Chen, C. Paranthoen, A. Fiore, C.Platz, and O. Gauthier-Lafaye, Appl. Phys. Lett. **82**, 1818 (2003).
6. E.A.Viktorov, P. Mandel,Y. Tanguy, J. Houlihan, and G. Huyet, Appl. Phys. Lett. **87**, 053113 (2005).
7. B. Tykalewicz, D. Goulding, S. P. Hegarty, G. Huyet, I. Dubinkin, N. Fedorov, T. Erneux, E. A. Viktorov, and B. Kelleher, Opt. Lett. **41**, 1034 (2016).
8. C. Wang, B. Lingnau, K. Lüdge, J. Even, and F. Grillot, IEEE J. Quantum Electron. **50**, 723 (2014).
9. B. Tykalewicz, D. Goulding, S. Hegarty, G. Huyet, D. Byrne, R. Phelan, and B. Kelleher, Opt. Lett. **39**, 4607 (2014).
10. M. Sciamanna and K. Panajotov, Phys. Rev. A **73**, 023811 (2006).
11. A. Hurtado, A. Quirce, A. Valle, L. Pesquera and M.J. Adams, Opt. Exp. **17**, 23637 (2009).
12. S. Osborne, P. Heinricht, N. Brandonisio, A. Amann and S. O?Brien, Semicond. Sci. Technol. **27**, 094001 (2012).
13. W. Coomans, S. Beri, G. Van der Sande, L. Gelens and J. Danckaert, Phys. Rev. A **81**, 033802 (2010).
14. A. Hurtado, M. Nami, I.D. Henning, M.J. Adams, L.F. Lester, IEEE J. Sel. Top. Quantum Electronics **19**, 1900708 (2013).
15. The device was designed to emit on a single mode in the GS via etched slots with a pattern tailored specifically to affect the GS modes. At the significantly removed wavelength of the ES, the pattern is essentially unseen and so the cavity modes are obtained as usual.
16. M. Gioannini, J. Appl. Phys. **111**, 043108 (2012).
17. M. Abusaa, J. Danckaert, E. A. Viktorov, and T. Erneux, Phys. Rev. A **87**, 063827 (2013).
18. L. Olejniczak, K. Panajotov, S. Wieczorek, H. Thienpont, M. Sciamanna, JOSA B **27**, 2416 (2010).
19. T. Habruseva, D. Arsenijević, M. Kleinert, D. Bimberg, G. Huyet and S.P. Hegarty, Appl. Phys. Lett. **104**, 021112 (2014).
20. O. Nikiforov, L. Jaurigue, L. Drzewietzki, K. Lüdge, and S. Breuer, Opt. Exp. **24**, 14301 (2016).

1. T. Erneux and P. Glorieux, "Laser Dynamics", Cambridge University Press, Cambridge, UK, 2010.
2. H. Kawaguchi, *"Bistabilities and Nonlinearities in Laser Diodes,"* Artech House, Norwood, MA (1994)
3. M. J. Adams, A. Hurtado, D. Labukhin, and I. D. Henning, Chaos **20** "Nonlinear semiconductor lasers and amplifiers for all-optical information processing," 037102 (2010).
4. I. White, R. Penty, M. Webster, Y. J. Chai, A. Wonfor, and S. Shahkooh, IEEE Commun. Mag., **40**, "Wavelength Switching Components for Future Photonic Networks," 74 (2002).
5. A. Markus, J. X. Chen, C. Paranthoen, A. Fiore, C.Platz, and O. Gauthier-Lafaye, Appl. Phys. Lett. **82**, "Simultaneous two-state lasing in quantum-dot lasers," 1818 (2003).
6. E.A.Viktorov, P. Mandel,Y. Tanguy, J. Houlihan, and G. Huyet, Appl. Phys. Lett. **87**, "Electron-hole asymmetry and two-state lasing in quantum dot lasers," 053113 (2005).
7. B. Tykalewicz, D. Goulding, S. P. Hegarty, G. Huyet, I. Dubinkin, N. Fedorov, T. Erneux, E. A. Viktorov, and B. Kelleher, Opt. Lett. **41**, "Optically induced hysteresis in a two-state quantum dot laser," 1034 (2016).
8. C. Wang, B. Lingnau, K. Lüdge, J. Even, and F. Grillot, IEEE J. Quantum Electron. **50**, "Enhanced Dynamic Performance of Quantum Dot Semiconductor Lasers Operating on the Excited State," 723 (2014).
9. B. Tykalewicz, D. Goulding, S. Hegarty, G. Huyet, D. Byrne, R. Phelan, and B. Kelleher, Opt. Lett. **39**, "All-optical switching with a dual-state, single-section quantum dot laser via optical injection," 4607-4610 (2014).
10. M. Sciamanna and K. Panajotov, Phys. Rev. A **73**, "Route to polarization switching induced by optical injection in vertical-cavity surface-emitting lasers," 023811 (2006).
11. A. Hurtado, A. Quirce, A. Valle, L. Pesquera and M.J. Adams, Opt. Exp. **17**, "Power and wavelength polarization bistability with very wide hysteresis cycles in a 1550nm-VCSEL subject to orthogonal optical injection," 23637 (2009).
12. S. Osborne, P. Heinricht, N. Brandonisio, A. Amann and S. O?Brien, Semicond. Sci. Technol. **27**, "Wavelength switching dynamics of two-colour semiconductor lasers with optical injection and feedback," 094001 (2012).
13. W. Coomans, S. Beri, G. Van der Sande, L. Gelens and J. Danckaert, Phys. Rev. A **81**, "Optical injection in semiconductor ring lasers," 033802 (2010).
14. A. Hurtado, M. Nami, I.D. Henning, M.J. Adams, L.F. Lester, IEEE J. Sel. Top. Quantum Electronics **19**, "Two-Wavelength Switching With a 1310-nm Quantum Dot Distributed Feedback Laser," 1900708 (2013).
15. The device was designed to emit on a single mode in the GS via etched slots with a pattern tailored specifically to affect the GS modes. At the significantly removed wavelength of the ES, the pattern is essentially unseen and so the cavity modes are obtained as usual.
16. M. Gioannini, J. Appl. Phys. **111**, "Ground-state power quenching in two-state lasing quantum dot lasers," 043108 (2012).
17. M. Abusaa, J. Danckaert, E. A. Viktorov, and T. Erneux, Phys. Rev. A **87**, "Intradot time scales strongly affect the relaxation dynamics in quantum dot lasers," 063827 (2013).
18. L. Olejniczak, K. Panajotov, S. Wieczorek, H. Thienpont, M. Sciamanna, JOSA B **27**, "Intrinsic gain switching in optically injected quantum dot laser lasing simultaneously from the ground and excited state," 2416 (2010).
19. T. Habruseva, D. Arsenijević, M. Kleinert, D. Bimberg, G. Huyet and S.P. Hegarty, Appl. Phys. Lett. **104**, "Optimum phase noise reduction and repetition rate tuning in quantum-dot mode-locked lasers," 021112 (2014).
20. O. Nikiforov, L. Jaurigue, L. Drzewietzki, K. Lüdge, and S. Breuer, Opt. Exp. **24**, "Experimental demonstration of change of dynamical properties of a passively mode-locked semiconductor laser subject to dual optical feedback by dual full delay-range tuning," 14301 (2016).